Spin-glass ordering in the diluted magnetic semiconductor $Zn_{1-x}Mn_xTe$

P. M. Shand* and A. D. Christianson
Physics Department, University of Northern Iowa, Cedar Falls, Iowa 50614

T. M. Pekarek
Physics Department, University of North Florida, Jacksonville, Florida 32224

L. S. Martinson and J. W. Schweitzer
Physics Department, University of Iowa, Iowa City, Iowa 52242

I. Miotkowski
Physics Department, Purdue University, West Lafayette, Indiana 47907

B. C. Crooker
Physics Department, Fordham University, Bronx, New York 10458

(Received 29 June 1998)

We have performed both ac susceptibility and dc magnetization measurements on the diluted magnetic semiconductor $Zn_{1-x}Mn_xTe$. The measurements clearly indicate spin-glass behavior. For samples with concentrations $x=0.51$ and $x=0.41$, the data for the imaginary part of the complex susceptibility (χ'') were analyzed according to conventional power-law dynamics and good scaling was obtained with the critical exponent values $z\nu=10\pm2$ and $\beta=1.0\pm0.2$. These values of $z\nu$ and β are consistent with results obtained in other insulating spin-glass systems with short-range interactions. Because of the presence of significant Dzyaloshinsky-Moriya anisotropy in these materials, an attempt was also made to fit the data using an activated dynamics model. However, the scaling of the χ'' data was less satisfactory in this case. Magnetization measurements on the $x=0.51$ sample also showed a spin-glass-like transition. Scaling of the nonlinear magnetization just above the transition gave $T_c=20.8\pm0.2$ K, and the critical exponent values $\gamma=4.0\pm1.0$ and $\beta=0.8\pm0.2$. The value of T_c obtained from the static magnetization measurements is in good agreement with the value $T_c=20.7\pm0.05$ K obtained from the dynamic scaling analysis. Further, the value for the critical exponent γ obtained in this work is in fair agreement with values reported for other spin-glass materials. These results represent convincing evidence that diluted magnetic semiconductors are a subset of the class of insulating spin-glass materials with short-range interactions.
[S0163-1829(98)02743-X]

I. INTRODUCTION

The low-temperature magnetic behavior of diluted magnetic semiconductor (DMS) spin systems has been of much interest for several years.[1–4] Recently, the prototypical DMS $Cd_{1-x}Mn_xTe$ has been the subject of continued theoretical and experimental investigations in an attempt to firmly establish that this material undergoes a continuous phase transition from paramagnetism to a spin-glass state.[5–12] If indeed $Cd_{1-x}Mn_xTe$ is a spin glass, then are all DMS alloys also spin glasses with the same critical exponents despite differences in exchange strengths and anisotropy?

$Cd_{1-x}Mn_xTe$ and other DMS alloys such as $Hg_{1-x}Mn_xTe$ and $Zn_{1-x}Mn_xTe$ are randomly site-disordered, semiconducting materials with short-range antiferromagnetic (superexchange) interactions between the Heisenberg spins. In these materials, both nearest-neighbor and next-nearest-neighbor interactions are antiferromagnetic. The existence of a spin-glass phase is noteworthy as the frustration mechanism in these materials is not due to competition between ferromagnetic and antiferromagnetic interactions.[13] Rather, the frustration is due to the geometrical properties of the fcc sublattice in which the antiferromagnetically coupled Mn ions reside.[5,14] In this respect, DMS spin glasses are distinct from ''canonical'' spin glasses such as AuMn and insulating spin glasses such as $Eu_xSr_{1-x}S$. Indeed, it has been suggested that DMS alloys are random-field antiferromagnets rather than spin glasses.[6] We shall return to this suggestion below.

Early studies of the ac susceptibility χ_{ac} in $Cd_{1-x}Mn_xTe$ and $Hg_{1-x}Mn_xTe$ showed that these materials have zero-frequency transition temperatures T_c that are greater than 0 K.[7–9] These data were analyzed on the basis of conventional dynamic scaling theory, which holds that the relaxation time τ diverges as a power law in the correlation length ξ, i.e., $\tau\sim\xi^z$. Here, z is a dynamic scaling exponent. Now, according to the static scaling hypothesis, $\xi\sim\varepsilon^{-\nu}$, where $\varepsilon=(T-T_c)/T_c$ and ν is a critical exponent. One therefore finds that

$$\tau\sim\varepsilon^{-z\nu}. \tag{1}$$

This so-called critical slowing down behavior has been found to provide an excellent description of the dynamics in the critical region above T_c.

An alternative description of the dynamics near the transition involving thermal activation over free-energy barriers has also been proposed.[5,7,8] In this case, for a free-energy barrier of height ΔF, the relaxation time is given by $\tau/\tau_0 = \exp(\Delta F/T)$, where τ_0 is the single-spin relaxation time. Further, the barrier height scales with the correlation length: $\Delta F \sim \xi^{\theta}$, with θ being a scaling exponent. These considerations lead to the logarithmic form

$$\ln(\tau/\tau_0) \sim (T - T_c)^{-\nu\theta}. \tag{2}$$

Attempts to scale the dynamic susceptibility data according to activated dynamics produced less convincing results than in the case of the critical slowing down description. These findings indicate that a continuous phase transition to a spin-glass state exists at finite temperatures in $Cd_{1-x}Mn_xTe$ and $Hg_{1-x}Mn_xTe$. Further, virtually identical critical exponents were obtained in both materials, which is expected since all DMS alloys should belong to the same spin-glass universality class.

To further test this hypothesis, we have made ac and dc magnetic susceptibility measurements on $Zn_{1-x}Mn_xTe$ alloys close to the spin freezing transition. The ac susceptibility χ_{ac} was measured for two samples with different x values. Both power-law and activated scaling analyses were applied to the data in order to determine which theory provides the better description of the behavior in the vicinity of the transition. Nonlinear dc susceptibility measurements in the region of the transitions were also made in order to compare the static scaling behavior of $Zn_{1-x}Mn_xTe$ with that of $Cd_{1-x}Mn_xTe$.

The $Zn_{1-x}Mn_xTe$ group of alloys was previously the only member of the telluride series of II-VI-based DMS materials in which the characteristics of the spin glass transition remained uninvestigated. Of the tellurides, $Zn_{1-x}Mn_xTe$ has the largest nearest-neighbor (NN) exchange strength J_1 ($J_1/k_B \approx -6.3$ K for $Cd_{1-x}Mn_xTe$ and -9.5 K for $Zn_{1-x}Mn_xTe$) (Refs. 1 and 15) and the largest Dzyaloshinsky-Moriya NN anisotropic exchange integral D_1. However, the ratio D_1/J_1 is approximately the same for both $Cd_{1-x}Mn_xTe$ and $Zn_{1-x}Mn_xTe$, with $D_1/J_1 \approx 0.054$.[15] (No data are available on the anisotropic exchange in $Hg_{1-x}Mn_xTe$.) $Zn_{1-x}Mn_xTe$ also has the smallest lattice parameter. These extreme values of exchange coupling and lattice parameters make $Zn_{1-x}Mn_xTe$ a prime candidate for the investigation of the characteristics of the spin freezing transition to test the hypothesis of universality.

Note that what are thought to be the key building blocks of the spin-glass transition, frustration and random dilution, are present in all II-VI DMS materials. Thus, if identical critical exponents are found in all the tellurides, then one can say with some confidence that all II-VI DMS alloys will exhibit the same critical point behavior, since other anion groups exhibit similar trends in the behavior of the exchange (isotropic and anisotropic) parameters.[1,15]

This paper is organized as follows. In Sec. II, the details of the experiments are presented. In Sec. III, the results are presented and discussed in two parts. Section III A deals with the ac susceptibility results, and the dc magnetization and nonlinear susceptibility are described in Sec. III B. Finally, the conclusions drawn for this work are given in Sec. IV.

II. EXPERIMENTAL DETAILS

The ac susceptibility measurements were performed on two single-crystal samples of $Zn_{1-x}Mn_xTe$ grown by the vertical Bridgman method. One sample had a mass of 98.2 mg and a nominal Mn concentration $x = 0.5$. A Curie-Weiss fit at high temperatures gave a concentration of $x = 0.51$. The measurements on this sample were carried out on a Quantum Design SQUID magnetometer with ac option. The in-phase (χ') and out-of-phase (χ'') components were simultaneously measured at an ac field strength of 3.5 Oe. The measuring frequencies were 0.1, 1, 10, and 100 Hz. The stability of the temperature during each measurement of χ' and χ'' was ± 0.05 K.

The other sample on which ac measurements were performed had a mass of 400 mg and a nominal x value of 0.4. A Curie-Weiss fit yielded a concentration of $x = 0.41$. The measurements were carried out with a LakeShore Model 7120 ac susceptometer, using an ac field strength of 12.5 Oe. To test for large-field nonlinearities, we also performed measurements at 10 Oe. No difference in the behavior of χ' or χ'' was detected at the lower field. The frequencies used in these measurements were 80, 225, 625, 1600, and 2300 Hz. In the temperature range of our measurements (11–22 K), the accuracy of the temperature calibration was ± 0.1 K. The stability of the temperature during each measurement of χ' and χ'' was ± 0.05 K.

The dc magnetization measurements were made on the same $x = 0.51$ sample mentioned above. The measurements were made with a Cryogenic Consultants Limited (CCL) SQUID magnetometer. Measurements were made for fields between 0 and 90 G (accounting for the remanent field of the superconducting magnet) and for temperatures between 5 and 300 K. Magnetization versus temperature data were taken at fixed fields beginning at a temperature below the cusp and ending when the nonlinear term had decayed to noise level. Temperature stability was achieved to within 0.01 K.

Finally, within the range of temperatures that the measurements were made, it was found that the temperature calibrations of the instruments agreed to within 0.3 K.

III. RESULTS AND DISCUSSION

A. ac susceptibility measurements

The dynamics of the transition are most sensitively probed by the measurement and analysis of $\chi''(\omega, T)$.[8] Figure 1 shows $\chi''(\omega, T)$ for several different frequencies for the $Zn_{0.49}Mn_{0.51}Te$ sample. Admittedly, the range of frequencies used in this study is rather limited, but is large enough to ensure the soundness of our conclusions. There is some scatter in the data because of the low level of the out-of-phase signal. Smoothing curves were therefore drawn through the data points in order to enable us to objectively determine the position of the peaks in the $\chi''(\omega, T)$ data. An examination of the behavior of $\chi''(\omega, T)$ allows us to discern whether critical slowing down or activated dynamics provides a better description of the dynamical characteristics of freezing transition in DMS systems.

In the critical slowing down description, $\chi''(\omega, T)$ behaves according to the scaling law[8,16]

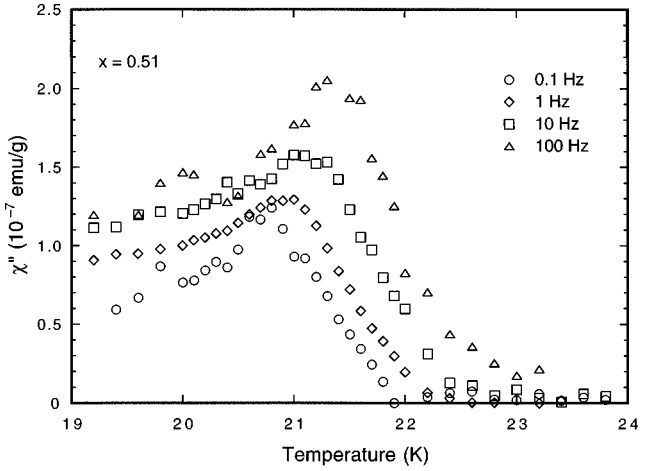

FIG. 1. Temperature dependence of χ'' near the freezing transition for $Zn_{0.49}Mn_{0.51}Te$. The measuring frequencies are 0.1, 1, 10, and 100 Hz. Through there is significant scatter in the data, the characteristic downward shift in the temperature at which the peak occurs as the frequency is decreased is evident.

$$T\chi''(\omega,T) \propto \varepsilon^{\beta} F(\omega\tau), \tag{3}$$

where β is the critical exponent for the order parameter, $F(x)$ is a universal function of x, and τ behaves according to Eq. (1). Equation (3) is completely general and is independent of the relaxation model used to derive it, but the form of the scaling function $F(x)$ is model dependent. However, as the critical point is approached, different model-dependent scaling functions should approach constant values. In addition, on the basis of an analysis of the spin autocorrelation function, Bertrand *et al.*[10] have argued that Eq. (3) is only valid for temperatures $T > T_p$, where T_p is the temperature at which the peak in $\chi''(\omega,T)$ occurs. We have taken this criterion into account in our analysis of all the $\chi''(\omega,T)$ data, which are shown in scaled form in Fig. 2. The data are well described by a single scaling curve. The best scaling was obtained for the following parameter values: $T_c = 20.7 \pm 0.1$ K, $z\nu = 10 \pm 2$, and $\beta = 1.0 \pm 0.2$. The determination of the best collapse of the data was made by first finding the best scaling by inspecting, which defined the region of the parameter space to be searched. The data were then fitted to a fourth-order polynomial and the χ-squared statistic calculated for each fit for a range of values of T_c, $z\nu$, and β. For a fixed value of T_c, the values of $z\nu$ and β were varied in turn and the behavior of χ squared examined. The minimum value of χ squared occurred most frequently at the values of $z\nu$ and β given above. For example, for a particular value of β (and T_c), as $z\nu$ is varied, the minimum in χ squared will most likely occur at $z\nu = 10$. Furthermore, the absolute smallest value of χ squared was obtained for the parameter values given above. Residuals were also checked to ensure that the best fits did not exhibit any pathological behavior. Fitting with a fifth-order polynomial produced no significant departure from the results given above. The uncertainties in the scaling exponents were obtained by ascertaining the extremal values of the parameters for which reasonably good scaling was still achieved. The uncertainties in $z\nu$ and β are rather large because of the relatively large uncertainties in the χ'' data. However, proper collapse of the data was very sensitive to changes in T_c.

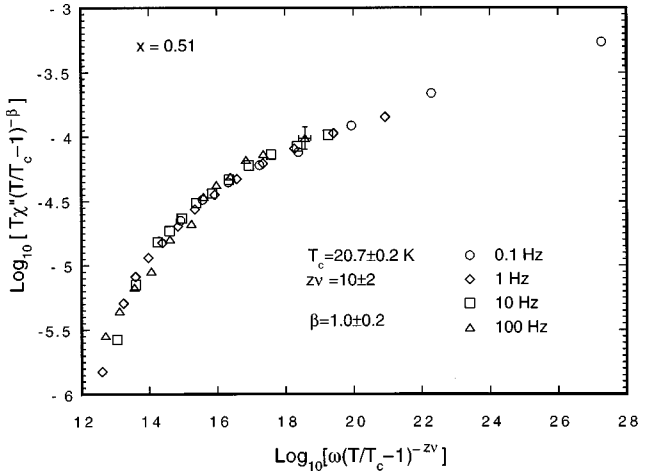

FIG. 2. Power-law scaling of the $\chi''(\omega,T)$ data for $Zn_{0.49}Mn_{0.51}Te$, according to Eq. (3) in the text. The frequencies are the same as those used in Fig. 1. The best-fit values of T_c and the scaling exponents $z\nu$ and β are also shown.

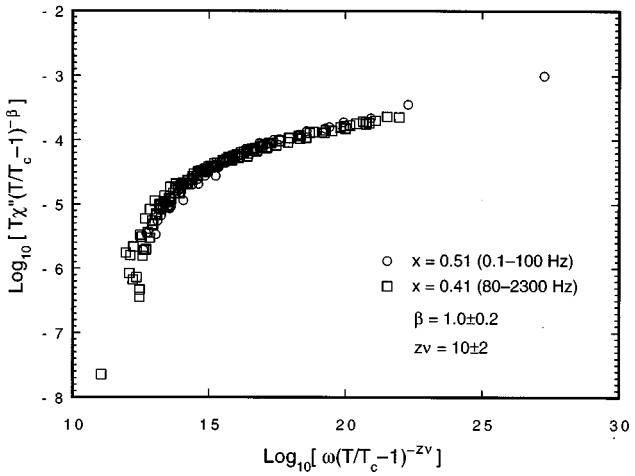

FIG. 3. Power-law scaling of the $\chi''(\omega,T)$ data for $Zn_{0.49}Mn_{0.51}Te$ and $Zn_{0.59}Mn_{0.41}Te$. For the $x = 0.51$ sample, $T_c = 20.7 \pm 0.1$ K and for the $x = 0.41$ sample, $T_c = 13.4 \pm 0.2$ K. To effect the overlap of the two data sets, the data for $Zn_{0.59}Mn_{0.41}Te$ have been shifted horizontally and vertically in the log-log plot to account for the difference in material-dependent factors (not explicitly shown) in the scaling expression Eq. (3).

In Fig. 3, a scaling plot that includes the $\chi''(\omega,T)$ data for both the $Zn_{0.49}Mn_{0.51}Te$ and $Zn_{0.59}Mn_{0.41}Te$ (Ref. 17) samples is shown. The critical exponent values $z\nu = 10 \pm 2$ and $\beta = 1.0 \pm 0.2$ have been used for both data sets. For the $x = 0.41$ sample, $T_c = 13.4 \pm 0.2$ K produced the best scaling. The two data sets overlap very well, indicating that the form of the scaling function F is independent of x, which further buttresses the critical slowing down description of the spin-glass transition. Note that to get the two data sets to overlap, the data for the $Zn_{0.59}Mn_{0.41}Te$ sample were normalized to those for the $Zn_{0.49}Mn_{0.51}Te$ sample in order to account for differences in material-dependent factors. This normalization amounted simply to shifting the $Zn_{0.59}Mn_{0.41}Te$ data horizontally and vertically in the log-log plot. In Fig. 4, a linear

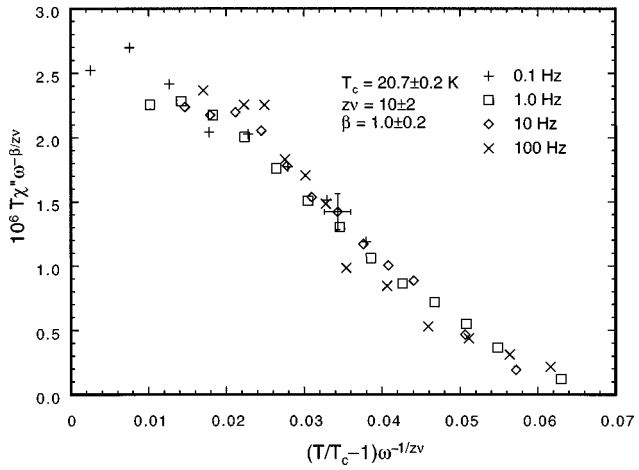

FIG. 4. Linear power-law scaling plot of the $\chi''(\omega,T)$ data for $Zn_{0.49}Mn_{0.51}Te$, according to Eq. (4). Scatter in the data is more apparent than in the log-log scaling plot, but reasonably good scaling is seen to be achieved.

scaling plot of the data for the $Zn_{0.49}Mn_{0.51}Te$ sample is shown according to the scaling form

$$T\chi''\omega^{-\beta/z\nu} \sim G(\varepsilon\omega^{-1/z\nu}), \tag{4}$$

which was proposed by Geschwind *et al.*[9] and represents a recasting of Eq. (3). The best-fit exponents given above are used in this plot. As expected, the linear plot fully exposes the effect of the scatter in the χ'' data. However, the scaling is still reasonably good, especially when one considers that the largest deviations are due to the 100 Hz χ'' data, which is the noisiest of all the data sets.

The values of the exponents $z\nu$ and β obtained in this work are clearly consistent with previous results obtained for $Cd_{1-x}Mn_xTe$ and $Hg_{1-x}Mn_xTe$. Similar values were also obtained in non-DMS insulating spin glasses. Table I summarizes the results obtained for critical exponents in a number of semiconducting and insulting spin-glass systems. Our results for $z\nu$ and β along with other listed in Table I strongly indicate that the same universal critical exponents indeed describe the spin-glass transition in all II-VI-based DMS materials. Further, though the consistency in the results is less compelling, the experimental evidence nevertheless points to DMS materials being a subset of a larger universality class of insulating spin glasses with short-range interactions.

TABLE I. Critical exponents for spin-glass systems.

Material	γ	β	$z\nu$
$Zn_{0.6}Mn_{0.4}Te$		1.0 ± 0.2*	10 ± 2*
$Zn_{0.5}Mn_{0.5}Te$	4.0 ± 1.0*	1.0 ± 0.2*	10 ± 2*
$Cd_{0.7}Mn_{0.3}Te$		0.8 ± 0.1[a]	9.25 ± 0.5[a]
$Cd_{0.6}Mn_{0.4}Te$	3.3 ± 0.3[b]	0.9 ± 0.2[b]	9.7[c]
$Cd_{0.62}Mn_{0.38}Te$		0.6 ± 0.1[d,e]	9 ± 1[d,e]
$Cd_{0.5}Mn_{0.5}Te$		0.6 ± 0.1[d,e]	9 ± 1[d,e]
$Hg_{0.7}Mn_{0.3}Te$		0.8 ± 0.1[a]	9.5 ± 0.5[a]
$Eu_{0.4}Sr_{0.6}S$		1.17 ± 0.1[f]	9 ± 1[f],7[g]
$SrCr_8Ga_4O_{19}$	2.1[h]		
$BaCO_6Ti_6O_{19}$		0.8 ± 0.1[i]	9.0 ± 0.5[i]
$Fe_{0.5}Mn_{0.5}TiO_3$	4.0 ± 0.3[j]	0.54[j]	10.5 ± 1.0[j]

*This work.
[a]Reference 8.
[b]Reference 12.
[c]Reference 7.
[d]Reference 29.
[e]Reference 11.
[f]Reference 16.
[g]Reference 30.
[h]Reference 27.
[i]Reference 31.
[j]Reference 24.

We have also attempted to interpret the $\chi''(\omega,T)$ data according to the activated dynamics description of the spin freezing transition. As mentioned in the Introduction, Geschwind *et al.* proposed that the dynamical slowing down indicated by the $\chi''(\omega,T)$ data was due to an inhibited transition to an ordered antiferromagnetic state.[6] This proposal was based on two factors: (i) anomalously large values of $z\nu(\approx 14)$ obtained when they fit their $\chi''(\omega,T)$ data for $Cd_{1-x}Mn_xTe$ according to the critical slowing down picture, and (ii) saturation of the antiferromagnetic correlation length near T_c as indicated by neutron diffraction results. The possible role of randomly directed Dzyaloshinsky-Moriya (DM) interactions was also discussed. As previously mentioned, it is now known that the strength of the NN DM interaction is about 5% of that of the NN isotropic superexchange interaction in both $Cd_{1-x}Mn_xTe$ and $Zn_{1-x}Mn_xTe$. Also, dipolar coupling is much weaker than the DM interaction in both materials.[15] Because the isotropic exchange coupling is antiferromagnetic and local DM anisotropy field is randomly directed, it is tempting to compare the freezing transition in $Cd_{1-x}Mn_xTe$ and $Zn_{1-x}Mn_xTe$ to a random-field transition such as that observed in $Fe_xZn_{1-x}Te$.[18–20] In these random-field Ising systems, the dynamical behavior in the critical region in the vicinity of the phase transition to the low-temperature ''frozen'' state is governed by activation over free-energy barriers resulting from competition between the random fields and the exchange. Hence, activated dynamics should be applicable, and is borne out by experiment.[18] The qualitative similarities between the random-field and random-axis anisotropy systems lead one to expect similar dynamical behavior near the transition to the frozen phase.[13] We have therefore analyzed our $\chi''(\omega,T)$ data based upon the assumption that the growth of the relaxation time is dictated by thermal activation, thus giving logarithmic frequency dependencies in the thermodynamic variables rather than the conventional power-law behavior.

In the activated dynamics picture, the scaling relation governing the behavior of $\chi''(\omega,T)$ near the transition can be written as[20,21]

$$\chi''(\omega,T) = \varepsilon^P G[-\varepsilon^Q \ln(\omega\tau_0)], \tag{5}$$

where P and Q are scaling exponents. If thermally activated excitations do indeed govern the critical dynamical behavior, then one expects the exponents P and Q to be universal for three-dimensional randomly disordered systems.[8] Figure 5 shows the best scaling plot corresponding to Eq. (5) for $Zn_{0.49}Mn_{0.51}Te$ data. This was obtained using these values: $T_c = 20.7\pm0.1$ K, $P = 1.0\pm0.2, Q = 0.4\pm0.1$, and $\tau_0 = 10^{-13}$ s. To obtain these best fit values, a large parameter space of values for P and Q was searched ($0.1 \leqslant P \leqslant 5$, $0.1 \leqslant Q \leqslant 5$). The scaling is apparently quite good. However, the highly compressed nature of the horizontal scale hides

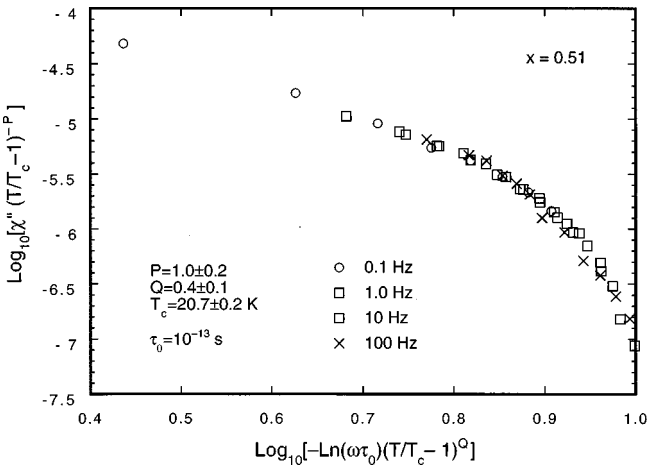

FIG. 5. Activated dynamic scaling of the $\chi''(\omega,T)$ data, according to Eq. (5) in the text. The best-fit values of the T_c, τ_0, and the scaling exponents P and Q are shown as well.

departures from good scaling, and a comparison of the χ-squared parameters for the power-law and activated scaling fits showed that better fits are obtained in the case of the conventional power-law description. The values of the exponents P and Q obtained for randomly-disordered magnetic systems are shown in Table II. The exponent values are certainly not as consistent as those shown in Table I, in which conventional critical dynamic scaling exponents are given. This lack of universality militates against the appropriateness of the activated dynamics description.

It should be noted that systems with random anisotropy are expected to exhibit induced Ising-like characteristics at criticality, which would lead one to expect a finite-temperature phase transition in three dimensions.[22,23] Such a finite-temperature transition is known to be well described by conventional critical slowing down.[24,25] Therefore, power-law dynamics is likely to hold in these cases. In reality, the Dzyaloshinsky-Moriya interaction strength is relatively weak in $Zn_{1-x}Mn_xTe$ and $Cd_{1-x}Mn_xTe$ as previously mentioned, and there is as yet no experimental evidence on the true role that the anisotropy in the spin-glass freezing.

TABLE II. Activated dynamics exponents for spin-glass systems.

Material	P	Q
$Zn_{0.5}Mn_{0.5}Te$	1.0 ± 0.2*	0.4 ± 0.1*
$Cd_{0.6}Mn_{0.4}Te$	0.65 ± 0.1[a]	0.65 ± 0.1[a]
$Cd_{0.35}Mn_{0.65}Te$	0.65 ± 0.1[a]	0.65 ± 0.1[a]
$Cd_{0.7}Mn_{0.3}Te$	3.65–4.2[b]	0.8[b]
$Hg_{0.7}Mn_{0.3}Te$	3.65–4.2[b]	1.2[b]
$Eu_{0.4}Sr_{0.6}S$	3 ± 1[c]	0.65[c]
$BaCo_6Ti_6O_{19}$	0.4 ± 0.1[d]	0.35 ± 0.05[d]

*This work.
[a]Reference 6.
[b]Reference 8.
[c]Reference 21.
[d]Reference 31.

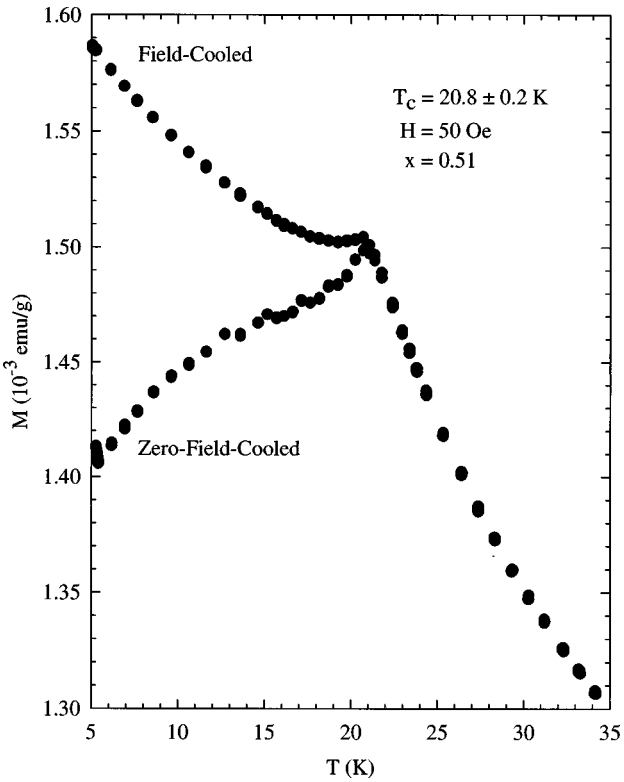

FIG. 6. Zero-field-cooled and field-cooled magnetization vs temperature T for $Zn_{0.49}Mn_{0.51}Te$. The cusp in the magnetization at $T=20.8\pm0.2$ K for the zero-field-cooled case is characteristic of a transition to the spin-glass phase.

B. Magnetization measurements

Magnetization measurements were made on the same $Zn_{0.49}Mn_{0.51}Te$ sample that was used in the ac measurements. Zero-field-cooled (ZFC) and field-cooled (FC) measurements in a 50-G field clearly show a freezing transition at a temperature of 20.8 ± 0.2 K, as seen in Fig. 6. Since the observed transition temperature is known to be suppressed from its asymptotic, zero-field limit,[26] we made a series of measurements in several low fields to verify that we were in the zero-field limit. We found that the transition temperature of 20.8 ± 0.2 K was independent (within experimental error) of the applied fields between 23 and 90 G. We therefore took this transition temperature to be the zero-field limit. Similar behavior was exhibited by the $Zn_{0.59}Mn_{0.41}Te$ sample. In a 20-G field, it showed a freezing transition at 13.6 ± 0.3 K, which is in good agreement with the independent ac susceptibility measurements.

We have also made nonlinear magnetization $M_{\rm nl}$ on the $Zn_{0.49}Mn_{0.51}Te$ sample close to the transition in order to examine the static scaling properties in the critical region. Just above the transition, the magnetization can be expanded as

$$M = a_1 H - a_3 H^3 + a_5 H^5 - a_7 H^7 \cdots, \tag{6}$$

where

$$\begin{aligned} M_{\rm nl} &= -a_3 H^3 + a_5 H^5 - a_7 H^7 + \cdots \\ &= -b_3 \varepsilon^{-\gamma} H^3 + b_5 \varepsilon^{-(2\gamma+\beta)} H^5 \\ &\quad - b_7 \varepsilon^{-(3\gamma+2\beta)} H^7 + \cdots \end{aligned} \tag{7}$$

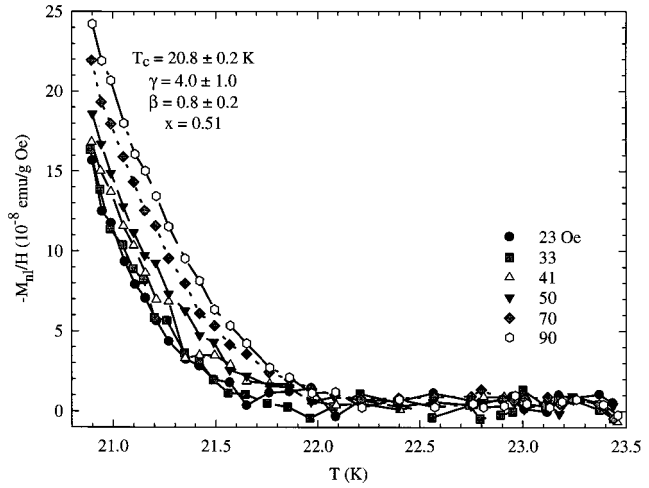

FIG. 7. Nonlinear susceptibility M_{nl}/H vs temperature T for $Zn_{0.49}Mn_{0.51}Te$ for several fixed fields. The divergence of the nonlinear term near T_c is expected near a spin-glass transition.

is the nonlinear magnetization, β is the same critical exponent discussed previously, and γ is another critical exponent.[12,27] A key characteristic of spin-glass materials is the divergence in $M_{\rm nl}/H$ as one approaches T_c from above. As pointed out by Mauger, Ferré, and Beauvillain, the expansion in Eq. (7), which predicts that the leading term should diverge as $\varepsilon^{-\gamma}$, is not valid for the region immediately around T_c.[12] In fact, the divergence of the nonlinear term is expected to soften in this regime due to the increasing importance of higher order terms. Instead, in the immediate vicinity of T_c, the universal scaling expression

$$M_{\rm nl}(\varepsilon,H)=\varepsilon^{(\gamma+3\beta)/2}F(H/\varepsilon^{(\gamma+\beta)/2}) \tag{8}$$

must be used. Note that the expansion of this scaling expression yields the previous expansion for $M_{\rm nl}$ [Eq. (7)] for the region above T_c where the nonlinear divergence begins.[12]

To examine the behavior of the magnetization near T_c, measurements of the magnetization as a function of temperature were made in several fixed fields. Near T_c, $\chi_{\rm nl}$ $=M_{\rm nl}/H$ increases as shown in Fig. 7, as would be expected if this quantity does indeed diverge at T_c. In Fig. 8, the data are plotted according to the universal scaling relation of Eq. (8) using values for the parameters γ, β, and T_c that produced the best scaling. The parameter values that produced the best scaling were $\gamma=4.0\pm1.0$, $\beta=0.8\pm0.2$, and $T_c=20.8\pm0.2$ K. The data collapse onto the single universal scaling curve that covers many orders of magnitude along both axes. For temperatures significantly greater than T_c (lower part of the curve), the slope approaches 3, consistent with the first-order term in Eq. (7). The scaling plot shows increasing scatter at higher temperatures since the nonlinear magnetization approaches zero as one moves out of the critical region. As T closely approaches T_c from above (upper part of the curve), the slope tends to the proper asymptotic value $(\gamma+3\beta)/(\gamma+\beta)$.[12] These asymptotic limits are shown as solid lines in Fig. 8.

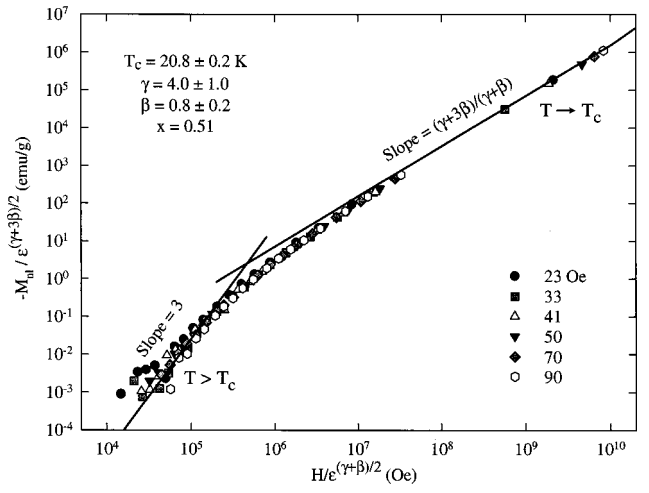

FIG. 8. The nonlinear magnetization data for $Zn_{0.49}Mn_{0.51}Te$ analyzed according to a universal scaling model for a spin-glass transition [Eq. (8) in the text]. The asymptotic limits for the slope, shown by the solid lines, are in agreement with the theory.

The value for the scaling exponent β obtained from the static scaling analysis is in accord with the value obtained from the dynamic scaling analysis discussed above, which reinforces the spin-glass picture. Previously reported values for γ as well as our own finding are also listed in Table I. The γ values range from 2.1 to 4.0. Comparing DMS systems, our value of $\gamma=4.0\pm1.0$ for $Zn_{0.49}Mn_{0.51}Te$ is slightly higher than the reported value of $\gamma=3.3\pm0.3$ for $Cd_{1-x}Mn_xTe$ found by Mauger, Ferré, and Beauvillain.[12] We note that the determination of γ via the scaling plot is very sensitive to slight changes in T_c, which explains the rather large error bars which we quote for our γ value. We comment that Geschwind and co-workers,[28] using linear scaling plots, found $\gamma=4.4$ in $Cd_{1-x}Mn_xTe$. This higher value of γ was debated by Bertrand *et al.*,[10] who suggested that the larger value of γ obtained by Geschwind *et al.* was due to the use of an incorrect value for T_c in the scaling plot. This debate notwithstanding, we conclude that within our experimental error, there is fair agreement between values for the critical exponent γ obtained in $Zn_{1-x}Mn_xTe$ and $Cd_{1-x}Mn_xTe$.

IV. CONCLUSION

By analyzing the imaginary part of the ac susceptibility $\chi''(\omega,T)$ for $Zn_{0.49}Mn_{0.51}Te$ and $Zn_{0.59}Mn_{0.41}Te$, we have shown that conventional critical slowing down gives a better description of the dynamics of the spin freezing transition in $Zn_{1-x}Mn_xTe$ than a thermal activation model. The values of the power law exponents obtained from the critical slowing down analysis were $z\nu=10\pm2$ and $\beta=1.0\pm0.2$. These values are in agreement with previous results obtained for $Cd_{1-x}Mn_xTe$ and $Hg_{1-x}Mn_xTe$, and also other insulating spin glasses with short-range interactions. Our attempt to describe the dynamic susceptibility data using an activated scaling Ansatz yielded exponent values $P=1.0\pm0.2$ and $Q=0.4\pm0.1$. When compared with values obtained for other similar systems, there is a marked lack of consistency, which militates against the idea of the universality of the activated dynamics exponents.

The magnetization of $Zn_{0.49}Mn_{0.51}Te$ shows a clear transition at $T=20.8\pm0.2$ K. Just above this transition, the nonlinear susceptibility $\chi_{\rm nl}$ diverges, which is consistent with

spin-glass behavior. From the scaling of the nonlinear magnetization just above the transition, we obtained the critical exponent values $\gamma = 4.0 \pm 1.0$ and $\beta = 0.8 \pm 0.2$, which are in fair agreement with the values reported for other spin-glass materials. We also note that the value $T_c = 20.8 \pm 0.2$ K obtained from the magnetization measurement is in very good agreement with the value $T_c = 20.7 \pm 0.1$ K obtained from the ac susceptibility analysis.

We therefore conclude that $Zn_{1-x}Mn_xTe$, like $Cd_{1-x}Mn_xTe$ and $Hg_{1-x}Mn_xTe$, undergoes an equilibrium phase transition to a spin-glass state. This strengthens the evidence that all II-VI-based DMS materials are true spin glasses characterized by the same critical exponents, and are probably a subset of a larger universality class of insulating spin glasses with short-range interactions.

ACKNOWLEDGMENTS

This research was supported by the Research Corporation and by National Science Foundation (NSF) Grant Nos. DMR-9221390, DMR-9318333, and DMR-9318385. Support from the Purdue Research Foundation is also gratefully acknowledged.

*Author to whom correspondence should be addressed. Fax: (319) 273-7136. Electronic address: Paul.Shand@uni.edu

[1] For a review of diluted magnetic semiconductors, see, J. K. Furdyna, J. Appl. Phys. **64**, R29 (1988).
[2] P. M. Shand, P. A. Polstra, I. Miotkowski, and B. C. Crooker, J. Appl. Phys. **75**, 5731 (1994).
[3] P. M. Shand, A. Lewicki, I. Miotkowski, B. C. Crooker, and J. K. Furdyna, Phys. Rev. B **44**, 6152 (1991).
[4] T. M. Pekarek, J. E. Luning, I. Miotkowski, and B. C. Crooker, Phys. Rev. B **50**, 16 914 (1994).
[5] A. Mauger, J. Villain, Y. Zhou, C. Rigaux, N. Bontemps, and J. Ferré, Phys. Rev. B **41**, 4587 (1990), and references therein.
[6] S. Geschwind, A. T. Ogielski, G. Devlin, J. Hegarty, and P. Bridenbaugh, J. Appl. Phys. **63**, 3291 (1988).
[7] A. Mauger, J. Ferré, M. Ayadi, and P. Nordblad, Phys. Rev. B **37**, 9022 (1988).
[8] Y. Zhou, C. Rigaux, A. Mycielski, M. Menant, and N. Bontemps, Phys. Rev. B **40**, 8111 (1989).
[9] S. Geschwind, David A. Huse, and G. E. Devlin, Phys. Rev. B **41**, 4854 (1990).
[10] D. Bertrand, A. Mauger, J. Ferré, and P. Beauvillain, Phys. Rev. B **45**, 507 (1992).
[11] B. Leclercq and C. Rigaux, Phys. Rev. B **48**, 13 573 (1993).
[12] A. Mauger, J. Ferré, and P. Beauvillain, Phys. Rev. B **40**, 862 (1989).
[13] For a review of spin-glass theory and experiments, see, for example, K. Binder and A. P. Young, Rev. Mod. Phys. **58**, 801 (1986).
[14] J. Villain, Z. Phys. B **33**, 31 (1979).
[15] B. E. Larson and H. Ehrenreich, Phys. Rev. B **39**, 1747 (1989).
[16] M. Continetino and A. P. Malozemoff, Phys. Rev. B **34**, 471 (1986).
[17] Complete $\chi''(\omega, T)$ data for $Zn_{0.59}Mn_{0.41}Te$ are presented in P. M. Shand, A. D. Christianson, L. S. Martinson, J. W. Schweitzer, T. M. Pekarek, I. Miotkowski, and B. C. Crooker, J. Appl. Phys. **79**, 6164 (1996).
[18] A. R. King, J. A. Mydosh, and V. Jaccarino, Phys. Rev. Lett. **56**, 2525 (1986).
[19] R. J. Birgeneau, Y. Shapira, G. Shirane, R. A. Cowley, and H. Yoshizawa, Physica B & C **137**, 83 (1986).
[20] D. S. Fisher, Phys. Rev. Lett. **56**, 416 (1986).
[21] A. P. Malozemoff and E. Pytte, Phys. Rev. B **34**, 6579 (1986).
[22] A. J. Bray and M. A. Moore, J. Phys. C **18**, L139 (1985).
[23] B. W. Morris, S. G. Colborne, M. A. Moore, A. J. Bray, and J. Canisius, J. Phys. C **19**, 1157 (1986).
[24] K. Gunnarson, P. Svedlindh, P. Nordblad, L. Lundgren, H. Aruga, and A. Ito, Phys. Rev. Lett. **61**, 754 (1988); Phys. Rev. B **43**, 8199 (1991).
[25] A. T. Ogielski, Phys. Rev. B **32**, 7384 (1985).
[26] See, for example, S. Oseroff and P. H. Keeson, in *Diluted Magnetic Semiconductors*, in Vol. 25 of Semiconductors and Semimetals, edited by J. K. Furdyna and J. Kossut (Academic, Boston, 1988).
[27] A. P. Ramirez, G. P. Espinosa, and A. S. Cooper, Phys. Rev. Lett. **23**, 2070 (1990).
[28] S. Geschwind, David A. Huse, and G. E. Devlin, Phys. Rev. B **41**, 2650 (1990).
[29] B. Leclercq, C. Rigaux, A. Mycielski, and M. Menant, Phys. Rev. B **47**, 6169 (1993).
[30] N. Bontemps, J. Rajchenbach, R. V. Chamberlin, and R. Orbach, Phys. Rev. B **30**, 6514 (1984).
[31] X. Battle, A. Labarta, B. Martinez, X. Obradors, V. Cabañas, and M. Vallet-Regí, J. Appl. Phys. **70**, 6172 (1991).